Surface Texture Improvement in the Turning Process Via Application of a Magnetostrictively Actuated Tool Holder

D. Liu

J. W. Sutherland

K. S. Moon

T. J. Sturos*

A. R. Kashani**

Department of Mechanical Engineering
and Engineering Mechanics,
Michigan Technological University,
Houghton, MI 49931-1295

An active vibration control system for a turning process is presented. The system employs a magnetostrictive actuator and a rate feedback control scheme to suppress the vibration caused by random excitation in the turning process. A specially designed tool holder is developed to implement the actuation and the control scheme effectively. A model which accounts for both the dynamic response of the cutting process and the control system is described. The effectiveness of the vibration control system is studied via simulation and a series of experiments. A disturbance force is applied to the system by a shaker and the dynamic response of the system is observed. The experimental data shows that the rate feedback control scheme adds additional damping to the system and reduces the vibration. A complete set of 2^4 factorial design cutting experiments were also conducted using the tool holder and experimentally obtained surface profiles were compared to surface profiles obtained without the vibration control. It is shown that the system can improve the surface texture generated by the turning process.

Introduction

Turning is one of the most common machining processes and has many applications. The dimensional accuracy and surface quality of a machined part are of primary importance in the turning process. It is known that the dimensional accuracy and surface quality are directly affected by dynamic displacement (vibration) between the tool and workpiece which arises during the cutting process. The vibration, particularly in the radial direction, is recognized to have a harmful effect on the machined surface texture (Moon and Sutherland, 1994). Although much progress has been achieved in reducing the vibration of machine tools through the improved design of machine tool structures, vibrations are still an important factor on the surface finish. Because of the small amplitude (several microns), wide bandwidth and random nature of machine tool vibrations, it is difficult to design passive vibration absorbers to suppress the vibrations for commercially available machine tools. Therefore, active vibration control, which applies an externally adjustable device (actuator) to provide a force to the vibrating structure, is attracting more and more attention from metal cutting practitioners and researchers.

Research to enhance the performance of machine tools through active control of machining operations is extensively reported in the literature. For the turning operation, much work has been performed to investigate the active control of cutting tool position for the purpose of process improvement. For example, Tsao and Tomizuka (1988, 1994) have explored the idea of changing the depth of cut during a turning operation. Specifically the depth of cut was varied using a hydraulic actuator to generate a non-cylindrical workpiece. Shiraishi et al. (1991) employed a stepping motor to actively control the chatter of the turning process. However, because the actuators used in these applications typically have low bandwidth, they are difficult to use for active vibration control of the machining process.

To overcome the limitations of the traditional actuators used in active vibration control, more and more attention is being focused on novel actuators made from "smart materials." The most commonly used materials now are piezoelectric ceramics. They have been used in many applications on machine tools (Liang and Perry, 1994; Dow, Miller and Falter, 1991; Okazaki, 1990). Another relatively new smart material is the magnetostrictive material. Although the magnetostrictive effect was discovered over a century ago, applications have recently begun to increase with the advent of Terfenol-D. Compared with piezoelectric ceramics, Terfenol-D has three advantages. While both materials can produce nearly instantaneous strain with relatively large force output, Terfenol-D's maximum strain available is larger than that of the piezoelectric ceramics. Second, Terfenol-D does not need the application of a high voltage like the piezoelectric material does, therefore it can be used in applications which are sensitive to electric charge. Third, the characteristics of Terfenol-D are much less temperature sensitive than those of the piezoelectric materials (Wang and Busch-Vishniac, 1992).

Magnetostrictive materials have been used in many applications such as sonar transducers and linear motors, but little has been reported on machine tool applications. The purpose of this paper is to present a magnetostriction-based micro-actuation system that can provide active, on-line manipulation of the cutting tool in the turning process. In this paper, a specially designed tool holder assembly with an integrated magnetostrictive actuator is introduced. A model describing the turning process and the actuation system is then developed. This model is then used to assist with the development of a rate feedback control scheme and a simulation study of the effectiveness of the system is presented. Following the simulation, the results from a series of cutting experiments are displayed and studied.

* Currently at Caterpillar Inc.

** Currently at University of Dayton, Dayton, OH.

Contributed by the Dynamic Systems and Control Division for publication in the JOURNAL OF DYNAMIC SYSTEMS, MEASUREMENT, AND CONTROL. Manuscript received by the DSCD February 21, 1995. Associate Technical Editor: Tsu-Chin Tsao.

Magnetostrictively-Actuated Tool Holder

The magnetostrictive effect, which was first discovered in Nickel by Joule in 1840, relates changes in the geometrical dimensions of a body to changes of a magnetic field applied to the body. A commercially available magnetostrictive material, Terfenol-D, is an alloy of terbium, dysprosium, and iron. The configuration of a typical magnetostrictive actuator is shown in Fig. 1. A rod of Terfenol-D provides a linear motion when it is excited by a magnetic field. A solenoid coil, driven by an external power supply, surrounds the rod and provides the necessary magnetic field. This magnetostriction is a transduction process in which electrical energy is converted into mechanical energy. Terfenol-D is an extremely brittle material and has a low tensile strength of about 28 MPa, but the compressive strength is much higher (700 MPa), so a push rod is used to ensure that the Terfenol-D material only bears a compression load. Another property of the Terfenol-D material is that larger elongations can be achieved by prestressing the material (Moffett et al., 1991). The actuator employed in this work (ETREMA NP50/6) uses a spring to produce a prestress in the material. The whole assembly is in an aluminum casing which is 100 mm in length and 34 mm in diameter. The maximum motion range of the actuator in this work is about 50 microns peak to peak and the maximum output force is 490 N. A current of more than 1.5 ampere would drive the Terfenol-D rod into the nonlinear range.

The side view of the tool holder which contains the magnetostrictive actuator is shown in Fig. 2. A simple flexor is used to transmit the motion of the actuator to the cutting tool. It has very little friction and reduces the mass of the moving part and the displacement transmission error. The flexor is designed to be stiff in the tangential and the longitudinal directions and flexible in the radial direction. The whole flexor structure was machined from a solid block of two inch thick aluminum. An accelerometer (PCB U353) is installed to measure the vibration of the tool in radial direction. A eddy current type displacement sensor (590-LG) and a force sensor (PCB M112) are also mounted to measure the displacement of the tool and force in radial direction. A preload bolt is used to adjust the preload on the actuator and to ensure that the actuator and tool are in constant contact. More information about the design considerations of the tool holder can be found in Michler et al. (1993).

Model Development for the Turning Process With the Tool Holder

In general, the vibration between tool and workpiece arises in three dimensional directions, however only the vibration in the radial direction is considered in this paper because it has the most detrimental effect on the surface finish of a turned part. To assist in the development of a control scheme for the tool holder, computer-based simulations of the system may be employed. The development of such a simulation requires a model for the dynamic response of the cutting process and tool holder. Considering the tool holder assembly as a lumped mass system, the structural dynamics of the system may be represented by a single degree of freedom system as shown in Fig. 3. In the figure, the nominal depth of cut for the turning operation is d_0, the feed is f, the spindle speed of the workpiece is N_s, the effective mass of the tool holder is m, the stiffness of the actuation system is k, and the damping coefficient of the system is c.

The radial force generated by the cutting process may be approximated as:

$$F_r = K_r f d_0 \tag{1}$$

where K_r is a scaling coefficient and fd_0 is the nominal chip load. Because of the nature of the turning process, material left uncut in the past revolution of the workpiece will increase the amount of material to be removed during the current revolution. The dependence of the chip load on both present and past displacements suggests that Eq. (1) should be modified to represent the radial force as:

$$F_r = K_r f(d_0 - x(t) + x(t - \tau)) \tag{2}$$

where $x(t)$ is the radial displacement at time t, $x(t - \tau)$ is the radial displacement at time $t - \tau$, and τ is the time required for one revolution of the workpiece.

Given the proceeding statements, the motion of the cutting tool can be described by a second-order differential equation:

$$m\ddot{x}(t) + c\dot{x}(t) + kx(t) = K_r f(d_0 - x(t) + x(t - \tau)) - u(t) \tag{3}$$

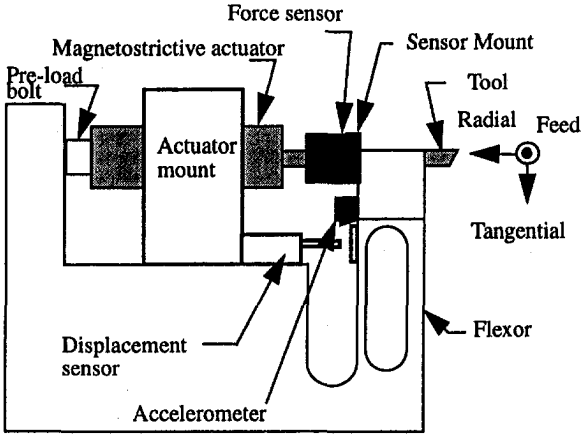

Fig. 2 Tool holder side view

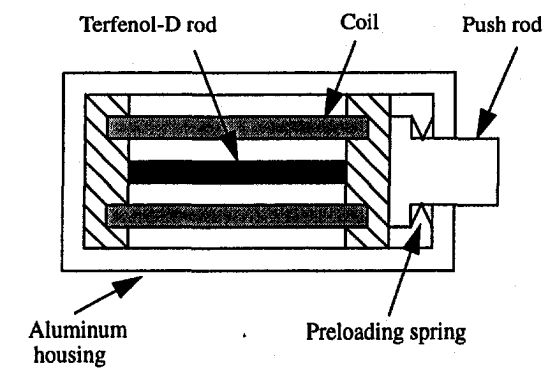

Fig. 1 Magnetostrictive actuator configuration

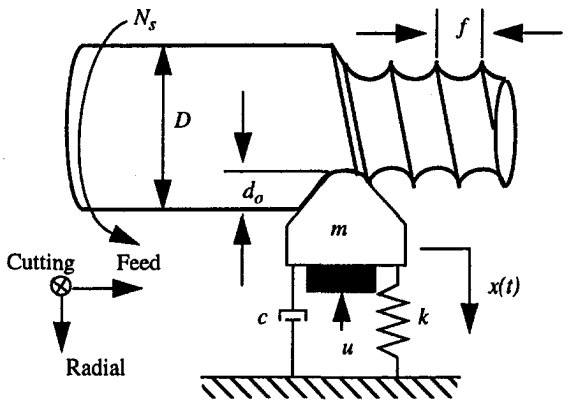

Fig. 3 Dynamic model of turning process with the tool holder

where $u(t)$ is the force applied to the mass of the tool holder by the actuator. The transfer function of Eq. (3) in the Laplace domain is

$$(ms^2 + cs + k)X(s) = K_r f(d_0 - X(s) + e^{-\tau s}X(s)) - U(s) \quad (4)$$

where $X(s)$ is the Laplace transform of the radial displacement and $U(s)$ is the Laplace transform of the output force generated by the actuator.

Because the actuator contains many of the same components as a motor, e.g., coil and electromechanical coupling, the output force, $U(s)$, may be described as

$$U(s) = \frac{K_u}{Ls + R} V(s) \quad (5)$$

where L is the coil inductance, R is the resistance of the coil, K_u is the force constant, and $V(s)$ is the Laplace transform of the voltage applied to the actuator. The model description above for the dynamic behavior of the tool holder and the turning process can be depicted by the diagram in Fig. 4. The block G in the diagram represents the adjustable gain of the power amplifier for the voltage used to control the actuator.

Parameter Identification for the Dynamics of the Tool Holder

From the preceding work, the dynamics of the magnetostrictive actuator based tool holder can be characterized as

$$\frac{X(s)}{V(s)} = \frac{K_a}{(\tau_1 s + 1)\left(\frac{s^2}{\omega_n^2} + \frac{2\zeta}{\omega_n} s + 1\right)} \quad (6)$$

where,

$\tau_1 = L/R$ is a time constant,
$\omega_n^2 = k/m$ is the natural frequency of the tool holder,
$\zeta = (1/2\omega_n)(c/m)$ is the system damping coefficient, and
$K_a = GK_u\tau_1/Lm\omega_n^2$ is the total gain of the actuation system.

The values of τ_1, ω_n, and ζ are, of course, very important to the dynamic performance of the tool holder and to the design of the controller. In order to obtain the value of these parameters, experiments were conducted to measure the frequency response of the tool holder.

A HP35660 dynamic signal analyzer was used to monitor the performance of the tool holder in the experiment. A periodic chirp signal of 0–3.6 kHz, produced by the source signal generator of the analyzer, was put into the tool holder through a power amplifier (MB Dynamic SS250VCF). This signal, which

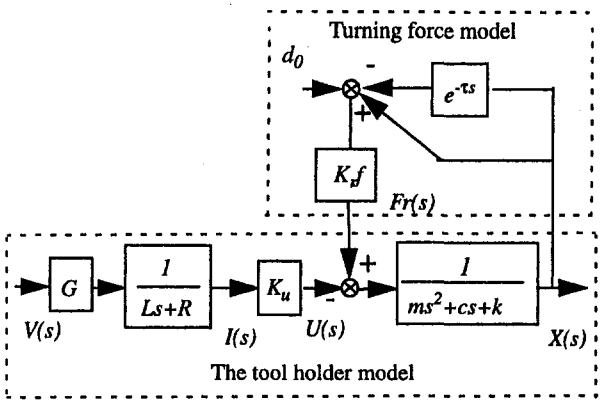

Fig. 4 Diagram of the dynamic model of the tool holder and the Turning Process

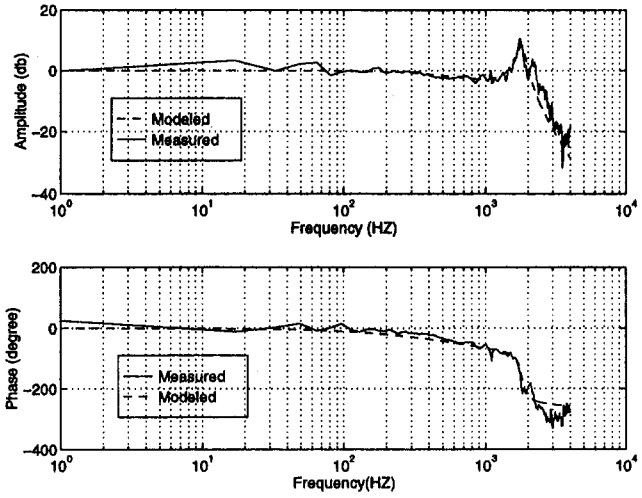

Fig. 5 Measured and modeled frequency response of the tool holder

is the input signal, was also sent to the analyzer. The displacement of the tool holder was collected by the eddy type displacement sensor (Indikon 590-LG) and was also fed into the dynamic signal analyzer. The analyzer could calculate the frequency response function of the tool holder at 400 data points. The measured FRF is shown in Fig. 5. The FRF shown in the figure is in fact the response of the power amplifier, the tool holder and the displacement sensor. However, since both the amplifier and the sensor are wide band electronic devices (bandwidth up to 20 kHz), it is reasonable to assume that they have effects only on the total gain of the system. This is also the reason that the amplitude of the FRF in Fig. 5 is plotted with unit dc gain.

A third order transfer function in the form of Eq. (6) was fit to the measured result and the parameters estimated were ω_n = 11373 rad/s, ζ = 0.06 and τ_1 = 0.27 ms. The predicted frequency response of the model with these estimated parameters is also shown in Fig. 5 as a dashed line.

Rate Feedback Control and Simulation Study

The experimental results depicted in Fig. 5 and discussed in the text indicate that the damping of the magnetostrictively-actuated tool holder is very small. The importance of damping in vibration suppression is well known. Therefore, a simple rate feedback control scheme is employed to increase the amount of damping in the system.

The key to the success of the rate feedback control is to measure the velocity accurately at the tool tip in the cutting process. Because of the limited space on the tool holder and the severe condition in cutting process (chips, heat, etc.), it is difficult to obtain the velocity signal directly. An accelerometer, however, can be easily mounted and secured to the tool holder. In this study, an acceleration signal is obtained and integrated to provide the velocity signal for the rate feedback control.

The use of an integrator to obtain the velocity signal from the acceleration signal can produce floating saturation during the integration process. To avoid this situation, this work employed a band pass filter to provide a rate signal based on the accelerometer output. The transfer function of the band pass filter is then:

$$K(s) = \frac{V(s)}{A(s)} = \frac{\omega_c^2 s}{s^2 + 2\zeta_c\omega_c s + \omega_c^2} \quad (7)$$

where $V(s)$ and $A(s)$ are voltage and acceleration in the Laplace domain, ζ_c is the compensator damping factor, and ω_c is the natural frequency of the band pass filter. In this research, a

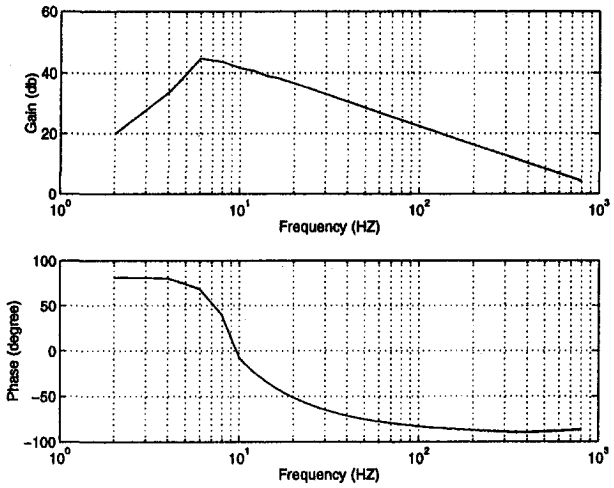

Fig. 6 The frequency response of the bandpass filter

band pass filter with $\omega_c = 37.7$ rad/s and $\zeta_c = 0.42$ was found to provide adequate performance.

Figure 6 shows the frequency response of the band pass filter. From the figure, it can be seen that the band pass filter acts as a differentiator for the frequencies below the cut off, but as an integrator for the frequencies above that. Because the vibration frequency in the turning process is generally much higher than the corner frequency (6 Hz), the band pass filter acts just as an integrator to the acceleration signal. The block diagram of the magnetostrictively-actuated tool holder with rate feedback is shown in Fig. 7.

In the model depicted in Fig. 7, if the closed turning force loop is stable, the tool vibratory motion will eventually settle due to the damping present in the machining process. Since the actual vibration signal does not settle to a single value, this suggests that process disturbances are present. In the absence of vibration, the machined work surface is determined solely by the geometry and kinematics of the turning process, however, process disturbances are present, and vibrations will always impact the machined surface texture (Zhang and Kapoor, 1991). The best that can be hoped for is to limit the extent to which the surface is affected by the process disturbances.

To check the ability of the rate feedback scheme to suppress vibration caused by random excitation, a simulation was performed using the turning model in combination with the tool holder model, as depicted in Fig. 7. The depth of cut, feed, and spindle speed used in the simulation were 0.76 mm, 0.075 mm, and 1000 rpm, respectively. The regenerative feedback term was approximated by a second order *Pade* model. A normally distributed disturbance was added to the nominal depth of cut. The disturbance had a zero mean with its deviation about 10 percent of the depth of cut. The variance of the tool displacement was used as the measurement of the vibration abatement. The performances of the rate feedback control scheme under different power amplifier gains was simulated and the results are listed in Table 1.

Table 1 Simulation result of rate feedback control

Gain	Variance
without control	0.7693
20	0.1186
40	0.0574
60	0.0352
80	0.0285
100	0.0238

From these simulation results, it was found that the suggested rate feedback control scheme effectively suppresses the vibratory motion caused by the random excitation. The results also show that the scheme is more effective with larger amplifier gains. The system did not become unstable with increasing gain, however, the effect of increasing the gain of the amplifier becomes smaller after the gain is about 40. These simulation results provided guidance for the cutting experiments to be described later.

Shaker Experiments

A series of experiments with a shaker (a vibration generator) were conducted to further examine the effectiveness of the tool holder with rate feedback control. The experimental setup is shown in Fig. 8. In the experimental setup, a shaker was employed to simulate the tool vibration for a cutting situation. The attachment of the shaker to the tool holder assembly provides a disturbance force in a manner intended to replicate actual cutting. An accelerometer is mounted between the shaker and the tool to monitor the vibration. The dynamic motion of the tool holder and the actuator are monitored via several sensors and a HP35670 frequency analyzer, which is used to capture the data and generate the frequency response functions. The system was examined with (closed-loop) and without (open-loop) rate feedback.

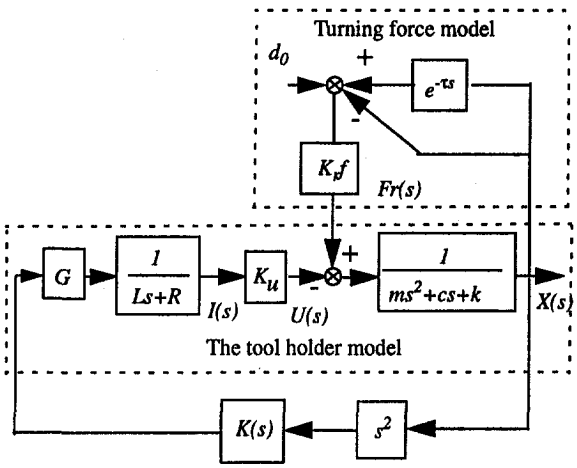

Fig. 7 The model of the tool holder with rate feedback

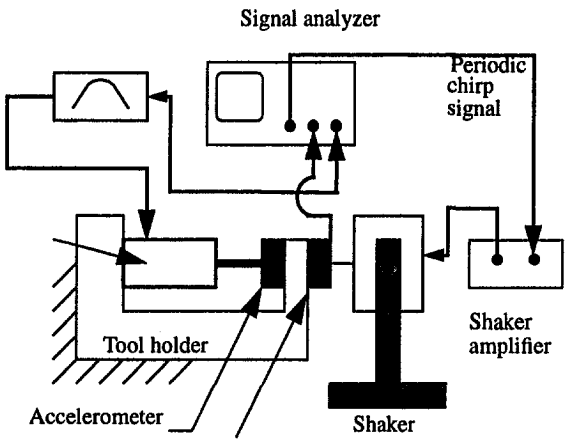

Fig. 8 Shaker experiment setup

For an open-loop test, the shaker introduces a disturbance force as a periodic chirp signal (bandwidth: 100 Hz–1700 Hz) to the tool holder assembly. In the experiment, the average of ten frequency response measurements is shown in Fig. 9 as a dashed line. The figure shows a resonance frequency (about 1150 Hz) in the system.

For the closed-loop test, the same conditions were applied as the open loop test. An MB250VCF power amplifier was used to drive the actuator. Combined with the open-loop frequency response in Fig. 9, the frequency response for the closed-loop experiment is shown with a solid line.

The comparison between the open-loop and the closed-loop tests shows that the rate feedback control scheme can suppress the vibration effectively. From the experimental result in Fig. 9, it is apparent that the peak has been removed. In fact, a maximum amplitude reduction of 14 dB has been achieved in the acceleration signal. The phase transition also shows a clear indication of additional damping in the system.

Cutting Experiments

Experiments were conducted to evaluate the performance of the actively controlled magnetostrictively-actuated tool holder under actual cutting conditions. Figure 10 shows the tool holder assembly mounted on the turret of a Cincinnati Milacron 850C turning center.

All the turning experiments employed an aluminum workpiece (6061-T6511) 56.5 mm in diameter and 153 mm in length. The K_r value for the material is about 1500 N/mm^2. A brand new carbide cutting tool with 0 deg side and back rake angles and 0.79 mm nose radius was used. The lead angle was 45 deg and the end cutting edge angle was 40 deg. While the simulation results suggested that the gain of the rate feedback control (i.e., the adjustable gain of the power amplifier) should be tuned as high as possible to obtain maximum vibration suppression, this was not confirmed by preliminary cutting experiments. These experiments showed that the magnetostrictively-actuated tool holder (MTH) became unstable (while cutting) for power amplifier gains over 95. It is postulated that this behavior may be due to the saturation nonlinearity of the displacement/magnetic field intensity relationship for the Terfenol-D actuator (note that this nonlinearity was not described within the simulation model). Based on the preliminary cutting experiments, the gain of the power amplifier was tuned to 80, to limit the input current to the magnetostrictive actuator to less than 1.5 A for subsequent cutting experiments.

Following the completion of the preliminary cutting experiments, a complete 2^4 factorial experiment was performed to study the effect of four factors on the machined surface texture. The four variables selected for study were depth of cut, spindle speed, feed, and control status (with or without rate feedback control). The experiments were conducted in a random order, and for each machined surface generated during the cutting experiments, surface profiles were collected using a stylus-type instrument (Perth-O-Meter). The profiles were collected by measuring along the axis of the workpiece. An A/D conversion board was employed to obtain digitized profile data from the instrument. The surface roughness values (R_a values) of all the profiles were calculated and are listed in the column labeled "R_a (μm) MTH" in Table 2. The data in the table may be used to judge the singular and joint effects of the variables on the surface roughness.

The surface profiles (with and without control) for a spindle speed of 500 rpm, a feed of 0.1 mm/rev and a depth of cut of 0.76 mm are shown in Fig. 11. The mechanism by which radial displacements are used in a surface profile generation is analogous to a sampling process and the sampling frequency is the spindle rotation frequency. This means that any time frequencies within the radial displacement signal are aliased into spatial frequencies within the surface profile. These frequency components manifest themselves as low spatial frequencies within the surface profile (Moon and Sutherland, 1994). It can be calcu-

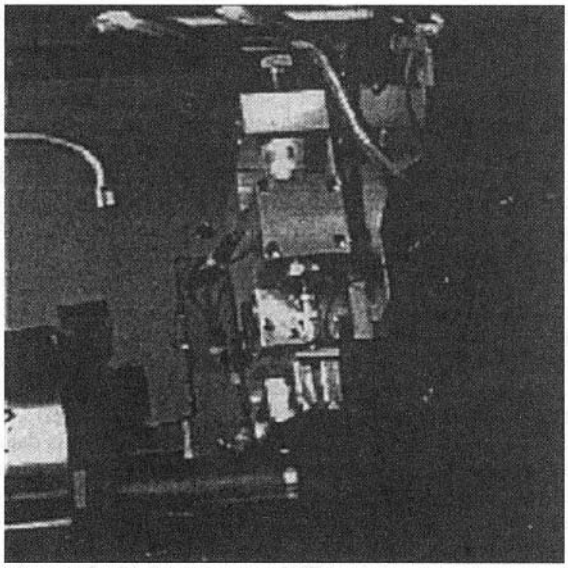

Fig. 10 The tool holder installed on a CNC turning center

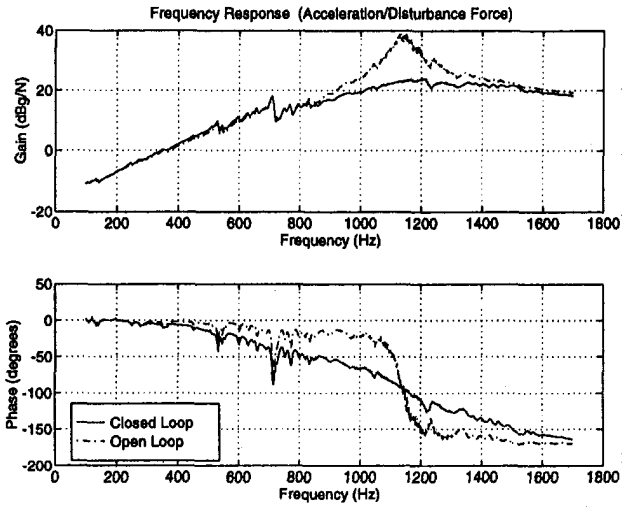

Fig. 9 Shaker experiment result (acceleration signal)

Table 2 R_a values of the surface cut in the experiment

C: Control status (with or without control)	S: Spindle speed (rpm)	F: Feed (mm/r)	D: Depth of cut (mm)	Ra (μm) MTH	Ra (μm) CTH
without	500	0.1	0.25	1.30	0.94
with	500	0.1	0.25	0.96	----
without	1000	0.1	0.25	1.21	1.07
with	1000	0.1	0.25	0.97	----
without	500	0.2	0.25	1.64	2.13
with	500	0.2	0.25	1.62	----
without	1000	0.2	0.25	1.56	2.19
with	1000	0.2	0.25	1.39	----
without	500	0.1	0.76	2.31	2.63
with	500	0.1	0.76	1.09	----
without	1000	0.1	0.76	2.77	0.94
with	1000	0.1	0.76	1.01	----
without	500	0.2	0.76	1.72	2.32
with	500	0.2	0.76	1.68	----
without	1000	0.2	0.76	1.90	2.71
with	1000	0.2	0.76	1.78	----

lated that the highest spatial frequency in the surface profile of Fig. 11 due to the radial vibration is 5 mm^{-1}, or the minimum wave length in the surface profile is 0.2 mm. The effect of the radial vibration abatement is expected as smaller amplitude low frequency undulations (wavelength longer than 0.2 mm) in the surface profile. Comparing the two surface profiles in Fig. 11, it can be seen that the surface profile obtained with rate feed back control (lower profile in the figure) appears to have smaller magnitude low frequency undulations than that obtained without control (upper profile).

Eight additional cutting experiments were performed under the same cutting conditions as with the magnetostrictively-actuated tool holder, but this time employing a conventional tool holder (ALORIS CXA 1). Surface profiles were also collected for these conventional tool holder (CTH) tests and the R_a values were calculated (listed in the column labeled "R_a (μm) CTH" in Table 2). Thus, Table 2 provides surface roughness data for eight unique cutting conditions under three tool holder conditions: conventional tool holder, controlled magnetostrictively-actuated tool holder, and magnetostrictively-actuated tool holder without control.

An examination of the MTH column in Table 2 reveals that the R_a values for the cutting conditions with rate feedback control are in every case lower than the corresponding conditions without control. To quantify this difference as well as to assess the significance of the singular and joint effects of the four variables producing the responses in the MTH column, the Analysis of Variance (ANOVA) of Table 3 was prepared.

Table 3 shows the Effect, Sum of Squares, Degrees of Freedom (DOF), and Mean Square for each variable as well as for each two-factor interaction between the four variables. The four factors considered are Control Status, Spindle Speed, Feed, and Depth of Cut, which are represented by capital letters C, S, F, and D, respectively, in the table. The Effects and Sum of Squares values were obtained using the standard techniques described by DeVor et al. (1992). A row in the table has been created for one of the three-factor interactions (between Control, Feed, and Depth of Cut) that was suspected to be significant. The other three-factor interactions and the four-factor interaction were then used to form the last row in the table, that is assumed to be due to experimental error. The F_{calc} values are the ratio of the Effect Mean Squares to the Error Mean Square. The displayed probability values (Prob.) are the probability of obtaining an F value larger than F_{calc} just due to chance.

For a significance level of 5 percent, the analysis indicated that both depth of cut and feed have significant effects on the surface roughness in the experiments. These results are to be

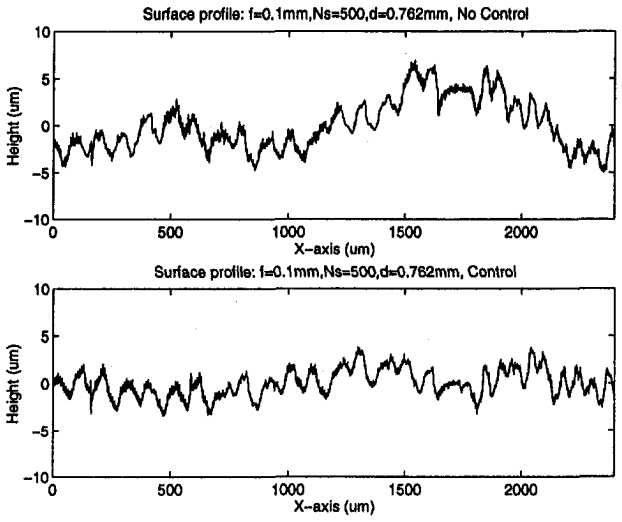

Fig. 11 A selected set of surface profiles

Table 3 ANOVA Table for MTH Data in Table 2

Source of Variation	Effect	Sum of Squares	DOF	Mean Square	F_{calc}	Prob.
C	-0.4888	0.95551	1	0.95551	68.71	0.001
S	0.0337	0.00456	1	0.00456	0.327	0.598
F	0.2088	0.17431	1	0.17431	12.53	0.024
D	0.4513	0.81451	1	0.81451	58.57	0.002
CxS	-0.0837	0.02806	1	0.02806	2.018	0.229
CxF	0.4013	0.64401	1	0.64401	46.31	0.002
SxF	-0.0413	0.00681	1	0.00681	0.489	0.523
CxD	-0.2963	0.35107	1	0.35107	25.24	0.007
SxD	0.1313	0.06891	1	0.06891	4.955	0.090
FxD	-0.2338	0.21857	1	0.21857	15.71	0.017
CxFxD	0.3038	0.36906	1	0.36906	26.54	0.007
Error		0.05563	4	0.01391		

C: control status; S: spindle speed; F: feed; D: depth of cut; □x□: interaction term; DOF: degree of freedom; F_{calc}: calculated F value; Prob.: probability of F_{calc}

expected. The control status variable was also judged to be significant, and in fact its effect size is comparable in magnitude to that of the depth of cut. The fact that the control variable is significant demonstrates the effectiveness of the control/actuation scheme.

One might reason that the effectiveness of the controlled tool holder should be judged relative to a conventional tool holder rather than an uncontrolled tool holder. It might be argued that the uncontrolled tool holder is much less rigid than a conventional tool holder and thus the experimental results demonstrate little about the advantages of the controlled tool holder. An examination of Table 3 suggests little difference on the average between the uncontrolled tool holder and the conventional tool holder. To test for a difference, if any, between the uncontrolled MTH and CTH R_a values a paired t-test analysis was performed. This analysis produced a t value of -0.0264 that may be compared to a t-distribution with seven degrees-of-freedom. Such a result indicates that there is no evidence to support the conjecture that the uncontrolled tool holder produces poorer surface finishes than the conventional tool holder. The similarity in performance between these two tool holders may be due to the relatively high stiffness of the Terfenol-D actuator (modulus of elasticity approximately one-half that of aluminum).

Another ANOVA table was constructed for a direct comparison of the controlled magnetostrictively-actuated tool holder and the conventional tool holder. This ANOVA produced comparable results to those displayed in Table 3. A paired t-test comparing the controlled tool holder and the conventional tool holder produced a statistically significant t value of -2.85 that should be compared to a t-distribution with seven-degrees-of-freedom. All these results indicate that the controlled tool holder produces a better surface finish than the conventional tool holder.

Conclusions

An actively controlled magnetostrictively-actuated tool holder for the turning process has been presented. The magnetostrictive actuator produces high force at nearly instantaneous speed and has good compressive strength. These properties make it very suitable for machining applications. A simple rate feedback control scheme was employed to add additional damping to the tool holder system. A model of the actuated tool holder combined with the turning process was developed and the simulation based on the model showed the effectiveness of the actuated tool holder in suppressing vibrations of the cutting tool.

A series of experiments were carried out to demonstrate the effectiveness of the proposed system. Shaker experiments showed that the rate feedback control scheme can add additional

damping to the system and a maximum amplitude reduction of 14 dB was obtained in the experiment. A 2^4 factorial design experiment that covers a wide range of cutting conditions was also conducted with both the magnetostrictively actuated tool holder and the conventional tool holder. Analysis of Variance and Paired t-test analysis were used to judge the surface finish data collected in the cutting experiments. The paired t-tests showed that the uncontrolled magnetostrictively actuated tool holder behaves just like a conventional tool holder. From the analysis of variance on the surface finish data, it is found that the magnetostrictively actuated tool holder with the rate feed back controller significantly improves the surface finish over both the conventional tool holder and the uncontrolled magnetostrictively actuated tool holder.

Acknowledgments

This research was sponsored in part by the NSF/ARPA Machine Tool Agile Manufacturing Research Institute (MT-AMRI) and the State of Michigan Research Excellence Fund program. Additional thanks are extended to PCB for their support in kind. The authors would like to thank William Kanizar (currently at Motorola, Inc.) for his assistance in the preparation of this manuscript.

References

DeVor, R. E., T. H. Chang, and J. W. Sutherland, 1992, *Statistical Quality Design and Control,* Macmillan, New York.

Dow, T. A., M. H. Miller, and P. J. Falter, 1991, "Application of a Fast Tool Servo for Diamond Turning of Nonrotationally Symmetric Surfaces," *Precision Engineering,* Vol. 13, No. 4, pp. 243–250.

Kiesewetter, L., 1988, "The Application of Terfenol in Linear Motors," Second International Conference on Giant Magnetostrictive and Amorphous Alloys for Actuators and Sensors, Marbella, Spain.

Liang, S. Y., and S. A. Perry, 1994, "In-Process Compensation for Milling Cutter Runout via Chip Load Manipulation," ASME *Journal of Engineering for Industry,* Vol. 116, No. 5, pp. 153–160.

Michler, J. R., K. S. Moon, J. W. Sutherland, and A. R. Kashani, 1993, "Development of a Magnetostriction Based Cutting Tool Micropositioner," *Transactions of NAMRI/SME,* Vol. 21, pp. 427–428.

Moffett, M. B. et al., 1991, "Characterization of Terfenol-D for Magnetostrictive Transducers," *Journal of Acoust. Soc. Am.,* Vol. 89, No. 3, pp. 1448–1455.

Moon, K. S., and J. W. Sutherland, 1994, "The Origin and Interpretation of Spatial Frequencies in a Turned Surface Profile," ASME *Journal of Engineering for Industry,* Vol. 116, No. 3, pp. 340–347.

Okazaki, Y., 1990, "A micro-positioning tool post using a piezoelectric actuator for diamond turning machines," *Precision Engineering,* Vol. 12, No. 3, pp. 151–156.

Shiraishi, M., K. Yamanaka, and H. Fujita, 1991, "Optimal Control of Chatter in Turning," *Int. J. Mach. Tools Manufact.,* Vol. 31, No. 1, pp. 31–43.

Sturos, T. J., J. W. Sutherland, K. S. Moon, D. Liu, and A. R. Kashani, 1995, "Application of an Actively Controlled Magnetostrictive Actuator for Vibration Abatement in the Turning Process," *Proceedings of ASME Dynamic Systems and Control Division,* DSC-Vol. 57-1, pp. 539–544.

Tsao, T. C., and M. Tomizuka, 1988, "Adaptive and Repetitive Digital Control Algorithms for Non-circular Machining," *Proceedings of American Control Conference,* Atlanta, GA, pp. 115–120.

Tsao, T. C., and M. Tomizuka, 1994, "Robust Adaptive and Repetitive Digital Tracking Control and Application to a Hydraulic Servo for Noncircular Machining," *Int. J. of Dynamic Systems, Measurement and Control,* Vol. 116, No. 3, pp. 24–32.

Wang, W., and I. Busch-Vishniac, 1992, "A high precision micropositioner based on magnetostrictive principle," Rev. Sci. Instr., Vol. 63, No. 1, pp. 249–254.

Zhang, G. M., and S. G. Kapoor, 1991, "Dynamic Generation of Machined Surfaces, Part 1: Description of a Random Excitation System," ASME *Journal of Engineering for Industry,* Vol. 113, pp. 137–144.

Zhang, G. M., and S. G. Kapoor, 1991, "Dynamic Generation of Machined Surfaces, Part 2: Contruction of Surface Topography," ASME *Journal of Engineering for Industry,* Vol. 113, pp. 137–144.